MOLECULAR AND CELLULAR BIOLOGY, Apr. 2007, p. 3044–3055 Vol. 27, No. 8
0270-7306/07/$08.00+0 doi:10.1128/MCB.02384-06
Copyright © 2007, American Society for Microbiology. All Rights Reserved.

Identification and Characterization of a Novel Component of the Human Minichromosome Maintenance Complex[▽]

Amos M. Sakwe,† Tin Nguyen,† Vicki Athanasopoulos, Kathy Shire, and Lori Frappier*

Department of Medical Genetics and Microbiology, University of Toronto, Toronto, Canada

Received 20 December 2006/Returned for modification 18 January 2007/Accepted 1 February 2007

Minichromosome maintenance (MCM) complex replicative helicase complexes play essential roles in DNA replication in all eukaryotes. Using a tandem affinity purification-tagging approach in human cells, we discovered a form of the MCM complex that contains a previously unstudied protein, MCM binding protein (MCM-BP). MCM-BP is conserved in multicellular eukaryotes and shares limited homology with MCM proteins. MCM-BP formed a complex with MCM3 to MCM7, which excluded MCM2; and, conversely, hexameric complexes of MCM2 to MCM7 lacked MCM-BP, indicating that MCM-BP can replace MCM2 in the MCM complex. MCM-BP-containing complexes exhibited increased stability under experimental conditions relative to those containing MCM2. MCM-BP also formed a complex with the MCM4/6/7 core helicase in vitro, but, unlike MCM2, did not inhibit this helicase activity. A proportion of MCM-BP bound to cellular chromatin in a cell cycle-dependent manner typical of MCM proteins, and, like other MCM subunits, preferentially associated with a cellular origin in G_1 but not in S phase. In addition, down-regulation of MCM-BP decreased the association of MCM4 with chromatin, and the chromatin association of MCM-BP was at least partially dependent on MCM4 and cdc6. The results indicate that multicellular eukaryotes contain two types of hexameric MCM complexes with unique properties and functions.

The initiation of DNA replication in eukaryotic cells is a carefully regulated process requiring the orchestrated assembly of many proteins at origin sites, including the origin recognition complex and minichromosome maintenance (MCM) complex. The MCM complex consists of six subunits, MCM2 through MCM7 (MCM2-7), which form a hexamer. Studies in *Saccharomyces cerevisiae*, where MCM proteins were first identified (25), showed that each of the MCM subunits performs an essential function in the initiation and elongation of DNA replication (20, 21). Genetic and biochemical studies conducted in yeast, *Xenopus*, *Drosophila*, and mammals point to probable roles of the MCM proteins in melting origin DNA and in functioning as the replicative helicase at replication forks (8, 27).

Biochemical analyses of the MCM complex have shown that MCM4, -6, and -7 are the most stably associated subunits, referred to as the helicase core (MCM4/6/7), with MCM2 and a dimer of MCM3 and MCM5 being more loosely associated with the core (13, 23, 30, 36). MCM4, MCM6, and MCM7 on their own can form hexamers with weak but measurable DNA helicase activity. The addition of MCM2 to the MCM4/6/7 core complex disrupts the hexamer and inhibits DNA helicase activity (12, 23). The complete MCM2-7 complex has no detectable helicase activity in vitro (12, 23), but helicase activity has been reported for a larger complex containing MCM2-7, cdc45, and GINS (29). As expected, MCM complexes exhibit ATPase activity (6, 23, 35). ATPase activity has not been observed in individual MCM subunits but occurs when certain pairs of MCM proteins interact (6).

Each of the six MCM subunits shares a region of homology referred to as the MCM box which contains the Walker A and Walker B ATPase motifs as well as an arginine finger motif (8, 17). Two additional proteins that contain an MCM box, like MCM2-7, have been identified in multicellular eukaryotes and named MCM8 and MCM9 (9, 14, 24, 39). MCM8 appears to function as a replicative DNA helicase independently from MCM2-7 (26), while the function of MCM9 is not yet clear. A protein named MCM10 is also important for DNA replication in eukaryotes, playing a role in priming DNA synthesis (7, 31). This protein lacks sequence homology to the other MCM proteins but, like MCM2-7, was identified in a yeast screen for genes essential for MCM (28).

While a great deal of evidence indicates the importance of the MCM2-7 complex in DNA replication, there are still unanswered questions concerning the functional roles of these MCM proteins. For example, while genetic evidence indicates a positive role in DNA replication for all the MCM subunits in the MCM2-7 complex, the helicase activity of the MCM4/6/7 subcomplex is actually inhibited by MCM2, -3, and -5. In addition, it is not clear why there are such high levels of the MCM proteins in cells, only a fraction of which maps to replication sites.

Recently, tandem affinity purification (TAP)-tagging methods have been developed that are well suited for the study of stable complexes in eukaryotic cells. Although this method was originally developed for use in yeast (32), we have found the approach to be extremely useful for detecting stable interactions in human cells when coupled with mass spectroscopy (10). A derivative of the classic TAP tag, called a sequential peptide affinity (SPA) tag, is similarly useful in identifying biologically important interactions (41). The SPA tag consists of a triple FLAG tag (3-FLAG) and a calmodulin binding peptide separated by a tobacco etch virus protease cleavage

* Corresponding author. Mailing address: 1 Kings College Circle, Toronto, Ontario, Canada M5S 1A8. Phone: (416) 946-3501. Fax: (416) 978-6885. E-mail: lori.frappier@utoronto.ca.

† A.M.S. and T.N. contributed equally to this work.

▽ Published ahead of print on 12 February 2007.

site, as opposed to the larger TAP tag combination of the protein A immunoglobulin G (IgG)-binding domain and calmodulin binding peptide. Both TAP- and SPA-tagged proteins can be purified from human cells under conditions where protein interactions are not disrupted. With the aim of learning more about MCM complexes in humans, we applied the TAP- and SPA-tagging systems to two of the core MCM subunits, revealing a previously unidentified interaction with an unstudied protein conserved in higher eukaryotes, referred to as MCM binding protein (MCM-BP).

MATERIALS AND METHODS

In vivo tagging experiments. The cDNA sequences encoding human MCM6 (kindly received from R. Knippers), MCM7 (kindly received from M. Ishibashi), or MCM-BP (purchased from ResGen-Invitrogen Corporation) were PCR amplified and cloned between the SalI and NdeI sites (MCM6) or between the XbaI and NotI sites (MCM7 and MCM-BP) of the ecdysone-inducible plasmid pMZI (41), such that the proteins were expressed fused to a C-terminal TAP tag. Dishes (150 mm) of 293T cells at 70% confluence were cotransfected with 8 μg of the pMZI construct and 8 μg of pVgRxR (Invitrogen) expressing the ecdysone receptor by calcium phosphate precipitation. At 15 h posttransfection, protein expression was induced by the addition of ponesterone A (Invitrogen), and TAP-tagged proteins were isolated from whole-cell lysates on IgG Sepharose and calmodulin Sepharose 4B resin as described in Holowaty et al. (10). MCM-BP and MCM2 (ResGen-Invitrogen Corp.) were also cloned between the XbaI and NotI sites of pMZS3F (41) in order to constitutively express these proteins fused to a C-terminal SPA tag. 293T cells in 150-mm dishes were transfected with 8 μg of pMZS3F-MCM-BP or pMZS3F-MCM2, and 48 h later SPA-tagged proteins were recovered from whole-cell lysates as for TAP-tagged proteins except that anti-FLAG M2 affinity resin (Sigma) was used instead of IgG Sepharose. Eluates were analyzed by sodium dodecyl sulfate-polyacrylamide gel electrophoresis (SDS-PAGE) and silver staining, and protein bands were identified by matrix-assisted laser desorption ionization—time of flight (MALDI-TOF) mass spectrometry as described in Holowaty et al. (10). For SPA-tagging experiments, bands were also identified by Western blotting using antibodies specific for individual MCM subunits (Santa Cruz) or rabbit serum raised against full-length MCM-BP purified as described below.

Coimmunoprecipitation. Log-phase HeLa cells were lysed in radioimmunoprecipitation assay (RIPA) buffer (50 mM Tris-HCl, pH 7.4, 1% NP-40, 0.1% sodium deoxycholate, 150 mM NaCl, 1 mM EDTA) or in RIPA buffer with 0.5% sodium deoxycholate where indicated, and clarified lysates were precleared for 1 h at 4°C with Protein A/G Plus agarose (Santa Cruz). Precleared lysates (1 mg) were incubated overnight at 4°C with 4 μg of control rabbit IgG (Santa Cruz), affinity-purified anti-MCM-BP rabbit antibody, anti-MCM7 rabbit antibody, or anti-MCM2 goat antibody (Santa Cruz), followed by a 2-h incubation with Protein A/G Plus beads and four washes in RIPA buffer. Proteins bound to the beads were then analyzed by Western blotting and probed with rabbit anti-MCM-BP, goat anti-MCM2, goat anti-MCM3, mouse anti-MCM4, rabbit anti-MCM5, or goat anti-MCM6 (all from Santa Cruz).

Analysis of recombinant MCM complexes in insect ells. Baculoviruses expressing each of the MCM subunits and MCM-BP were generated after cloning each cDNA into pFastBacHT (Pharmingen/BD Biosciences) and generating bacmids that were used to transfect *Spodoptera frugiperda* (Sf9) insect cells. cDNAs for MCM2, MCM3, MCM4, and MCM5 were purchased from ResGen-Invitrogen Corp. Constructs were made such that each protein (except MCM2) contained an N-terminal six-histidine tag, and some constructs also contained a StrepII tag (MCM4), a hemagglutinin tag (MCM6), or a 3-FLAG tag (MCM7) following the six-histidine tag. MCM2 contained either a C-terminal six-histidine or C-terminal StrepII tag. Baculoviruses expressing MCM3, MCM4, MCM5, and MCM6 without tags were also generated. High Five insect cells were coinfected with amounts of baculovirus determined to give optimum protein expression and harvested 3 days postinfection. To generate hexameric complexes, His-FLAG-MCM7 was coexpressed with either MCM2-His or His-MCM-BP and with a nontagged version of MCM3-6. Cells were lysed in 50 mM HEPES, pH 7.5, 150 mM NaCl, 10 mM imidazole, 1% Triton X-100, and complete protease inhibitor mixture (Sigma), and proteins were applied to nickel resin and eluted with 250 mM imidazole. Eluted proteins were incubated with anti-FLAG resin and eluted with 0.5 mg/ml 3-FLAG peptide (Sigma). Eluates were analyzed by SDS-PAGE and silver staining, and individual bands were identified by MALDI-TOF mass spectrometry and Western blotting. For tetrameric complexes of MCM4/6/7 with MCM2 or MCM-BP (see Fig. 5B), His-FLAG-MCM7 was coexpressed with the three other MCM proteins, and MCM7-containing complexes were isolated by incubating cell lysates (generated as above) directly with anti-FLAG resin. Proteins were eluted with FLAG peptide and analyzed by SDS-PAGE and silver staining. Complexes of MCM4/6/7 were also generated by coexpression of His-FLAG-MCM7 with MCM4 and MCM6. These cell lysates were mixed with lysates from insect cells expressing either MCM2 or MCM-BP and incubated for 30 min on ice. The mixed lysates were then applied to FLAG resin, and retained proteins were eluted and analyzed as above.

Purification of MCM-BP and MCM2. High Five insect cells were infected with baculovirus expressing His-MCM-BP or MCM2-His, harvested 3 days later, and lysed in 50 mM NaH_2PO_4, pH 8.0, 300 mM NaCl, 5 mM imidazole, 1% NP-40 and complete protease inhibitor mixture (Sigma). The clarified lysate was loaded onto a Ni-nitrilotriacetic acid (NTA) column (QIAGEN), washed with 10 mM imidazole, and eluted with 250 mM imidazole. After a dialyzing step against buffer A [50 mM Tris, pH 8.0, 150 mM NaCl, 0.1 mM EDTA, 0.1 mM 4-(2-aminoethyl)-benzenesulfonyl fluoride HCl (AEBSF),10% glycerol], the proteins were loaded onto a Superdex 200 gel filtration column. Peak fractions were collected and concentrated by loading on a MonoQ column, eluting in buffer A containing 500 mM NaCl, and dialyzing against buffer A.

Purification of the MCM4/6/7 core complex. High Five cells were coinfected with baculoviruses expressing His-StrepII-MCM4, His-hemagglutinin-MCM6, and His-FLAG-MCM7. After 72 h, the cells were harvested, washed twice with phosphate-buffered saline (PBS), and lysed in 10 volumes of 50 mM HEPES (pH 7.5), 300 mM NaCl, 10 mM imidazole, 10% glycerol, 1% Triton X-100, and complete protease inhibitors (Sigma). The lysate was clarified by centrifugation at 30,000 × *g* for 30 min and then loaded on an Ni-NTA column. The bound protein was eluted with 50 mM HEPES (pH 7.5), 300 mM NaCl, 250 mM imidazole, 10% glycerol, and complete protease inhibitors. Eluted protein was mixed with anti-FLAG M2 resin for 1 h at 4°C. The resin was washed three times with 50 mM HEPES (pH 7.5), 300 mM NaCl, 0.1 mM EDTA, and 10% glycerol, and bound protein was eluted with 5 column volumes of 0.5 mg/ml 3-FLAG peptide (SIGMA). Eluates were applied to StrepT-actin resin (QIAGEN), and MCM4/6/7 complexes were eluted with 5 mM desthiobiotin.

Glycerol gradient analysis. High Five cells were coinfected with baculoviruses expressing MCM4, MCM6, His-FLAG-MCM7, and either His-MCM-BP or MCM2-His. Lysates were generated, and proteins were isolated on Ni-NTA and anti-FLAG resin as described above and then loaded onto a 12-ml 15 to 35% glycerol gradient in 20 mM Tris-HCl, pH 7.5, 100 mM NaCl, 0.1 mM EDTA, 0.01% Triton X-100, and 1 mM AEBSF. After centrifugation at 34,000 rpm in an SW41 rotor for 16 h at 4°C, 23 500-μl fractions were collected from the top of the gradient and analyzed by SDS-PAGE and silver staining. The sedimentation of His-MCM-BP alone (purified on nickel resin) and glycerol gradient standards (Amersham) were also analyzed on gradients identical to those used for the MCM complexes.

DNA helicase assays. DNA helicase assays were conducted using a substrate that consisted of a ^{32}P-end-labeled 17-mer oligonucleotide (5′-GTTTTCCCAG TCACGAC-3′) annealed to single-stranded M13mp18 (NEB) (12). The annealed substrate was purified using a microSpinS-400 HR column prior to use (Amersham). A total of 1.5 fmol of labeled DNA substrate was incubated with 0.5 pmol of highly purified MCM4/6/7 complex with or without purified MCM2 or MCM-BP (2 to 10 pmol) at 30°C for 60 min in a 30-μl reaction mixture containing 10 mM HEPES, pH 7.5, 10 mM magnesium acetate, 50 mM NaCl, 1 mM DTT, 6 mM ATP, and 0.1 mg/ml bovine serum albumin. The reaction was stopped by the addition of 6 μl of 5×stop solution (100 mM EDTA, 0.5% SDS, 0.1% xylene cyanol, 0.1% bromophenol blue, 25% glycerol, 2 mg/ml proteinase K), and products were analyzed by 12% PAGE, followed by autoradiography.

Immunofluorescence imaging. The localization of endogenous MCM-BP and MCM6 or MCM4 was compared in HeLa cells. Cells were either fixed directly in 3% paraformaldehyde or extracted in mCSK buffer (10 mM PIPES [piperazine-*N*,*N*′-bis(2-ethanesulfonic acid)], pH 6.8, 100 mM NaCl, 300 mM sucrose, 1 mM $MgCl_2$, 1 mM EGTA, 1 mM dithiothreitol, 0.1% Triton X-100, and protease inhibitor mixture) followed by paraformaldehyde fixation. Samples were then stained with affinity-purified rabbit anti-MCM-BP antibody (1:50 dilution) and either purified goat anti-MCM6 or monoclonal anti-MCM4 antibodies (Santa Cruz), followed by fluorescein isothiocyanate-conjugated donkey anti-rabbit (Santa Cruz) and either Texas Red-conjugated goat anti-mouse or Texas Red-conjugated donkey anti-goat secondary antibodies (Chemicon, Temecula, CA). Cells were counterstained with DAPI (4′,6′-diamidino-2-phenylindole) and visualized at 400-fold magnification using a Leica DMIRB2 inverted epifluorescence microscope equipped with a digital cooled charge-coupled device camera and OpenLab, version 4.0, image capturing software (Improvision Inc., Lexington, MA).

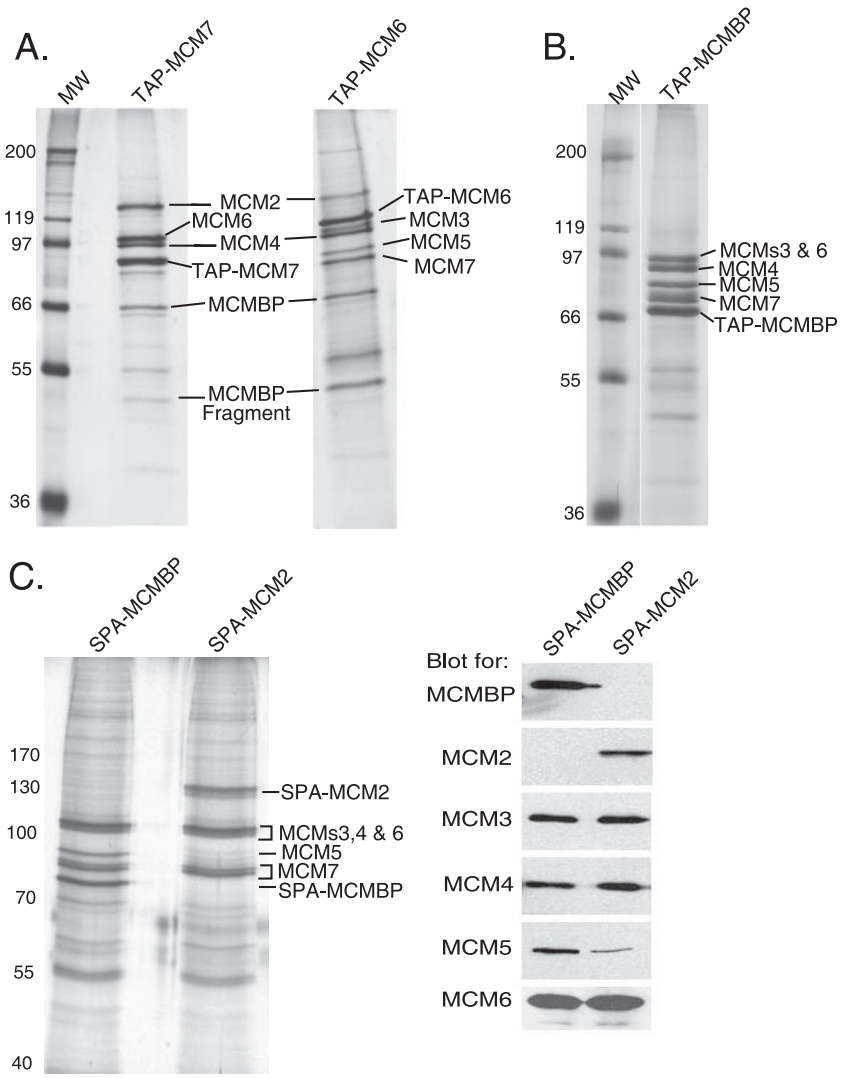

FIG. 1. TAP tagging of MCM proteins in human cells. (A) MCM7 or MCM6 was expressed in human cells fused to a TAP tag and then was isolated from cell lysates on IgG and calmodulin affinity resins. The final eluates were analyzed by SDS-PAGE and silver staining. Individual bands were excised and identified by MALDI-TOF mass spectrometry. The unlabeled band running at 60 kDa was identified as hsp60. (B) The experiment in panel A was repeated with the modification that MCM-BP was TAP tagged. (C) MCM-BP or MCM2 was expressed in human cells fused to a SPA tag and then was isolated from cell lysates on anti-FLAG and calmodulin affinity resins. Seventy-five percent of each sample was compared by SDS-PAGE and silver staining, and the individual bands were identified by MALDI-TOF mass spectrometry. Twenty-five percent of each sample was analyzed separately by SDS-PAGE and then transferred to a filter for Western blotting using antibodies specific for MCM2, -3, -4, -5, or -6 or MCM-BP, as indicated. MW, molecular weight.

Cell fractionation experiments. HeLa cells were blocked either at G_1/S or G_2/M by treatment of serum-starved cells with 10 μM aphidicolin (Sigma) or 20 μM nocodazole (Sigma), respectively, for 14 to 16 h. G_1/S cells were washed and grown without aphidicolin for 3 or 6 h to generate S-phase cells. Nocodazole-blocked cells were separated into G_2 (attached to plate) and early M (detached from plate) cells as previously described (2). Late M cells were generated by harvesting nocodazole-blocked early M cells by mitotic shake-off and culturing them for 3 h without nocodazole. Synchronization of the cells was verified by flow cytometry analysis of DNA content following propidium iodide staining, and G_2 and early M populations were further verified by immunoblotting for phosphorylated histone H3 to show that histone H3 is phosphorylated in the early M but not the G_2 cells (data not shown). Cells were then lysed and fractionated into soluble and chromatin-bound fractions as previously described (33). Briefly, cells were lysed in hypotonic buffer (10 mM HEPES pH 7.9, 10 mM KCl, 1.5 mM $MgCl_2$, 0.34 M sucrose, 10% glycerol, 1 mM dithiothreitol, 1 mM phenylmethylsulfonyl fluoride, and 0.04% Triton X-100); then soluble proteins were separated from extracted nuclei by centrifugation at 2,000 × *g* for 4 min. Chromatin-associated proteins were extracted from the nuclear pellet fraction with RIPA buffer and then clarified by centrifugation at 16,000 × *g* for 10 min to obtain the solubilized chromatin-associated proteins. Equal amounts of the soluble and chromatin-associated protein fractions were compared by SDS-PAGE and immunoblotting. In some cases MCM-BP expression was down-regulated prior to cell synchronization using the small interfering RNA (siRNA) TTGGGATTGT TTCAAAGTAAA (QIAGEN). HeLa cells (30 to 50% confluent) in six-well plates were transfected with 50 pmol of siRNA for MCM-BP, or GFP22 siRNA (QIAGEN) against green fluorescent protein (GFP) as a negative control using Lipofectamine 2000 according to manufacturer's instructions (Invitrogen). At 48 h posttransfection, the cells were synchronized as described above. In cases where MCM4 was silenced, 100 pmol of a mixture of three siRNAs (sc-37619 from Santa Cruz) was used to transfect HeLa cells as described above. Similarly, cdc6 was silenced using 100 pmol of a mixture of four siRNAs (sc-29258 from Santa Cruz).

ChIP assays. S-phase HeLa cells were generated by aphidicolin treatment, followed by a 6-h release. G_1 cells were generated by serum starvation for 48 h,

followed by a 6-h release in complete medium. Cells were fixed in PBS containing 1% formaldehyde for 15 min at room temperature. The unreacted formaldehyde was quenched with 125 mM glycine in PBS, and the fixed cells were harvested. Chromatin-enriched fractions were prepared as described above and fragmented by enzymatic shearing according the manufacturer's instructions (Active Motif), followed by brief sonication and centrifugation at 16,000 × *g* for 10 min at 4°C. Chromatin immunoprecipitation (ChIP) assays were performed essentially as described previously (33) using 2 μg of antibodies to MCM-BP, MCM2, and MCM4, control normal rabbit IgG (Santa Cruz) in RIPA buffer, and 50 μg of sheared DNA. After elution from the Protein A/G Plus beads and reversal of the cross-links, the chromatin was purified on QIAprep spin columns (QIAGEN). Quantitative real-time PCR was performed with 1/50 to 1/100 of the ChIP DNA template and Platinum SYBR Green qPCR SuperMix-UDG (Invitrogen) in a Rotorgene qPCR System (Corbett Research). The primer pairs used were LB2-F and LB2-R for the lamin B2 origin (LB2), LB2C1-F and LB2C1-R for the lamin LB2C1 fragment (approximately 4 kb from the origin), and LB2C2-F and LB2C2-R for the lamin LB2C2 fragment (approximately 3 kb from the origin on the opposite side from LC2C1) as shown in Ladenburger et al. (22). The recovery of the amplified DNA fragments with protein-specific and control IgG antibodies was calculated using the Rotorgene 6 software package (Corbett Research), normalized to the input DNA (eluted chromatin before immunoprecipitation), and then expressed as the relative increase (*n*-fold) over control IgG.

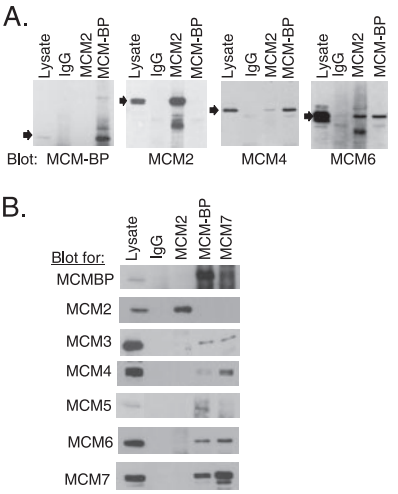

FIG. 2. Coimmunoprecipitation of endogenous MCM proteins. HeLa whole-cell lysates were incubated with antibodies against MCM2, MCM-BP, MCM7, or negative control IgG (IgG) as indicated on the top of each blot. Immunoprecipitants were analyzed by Western blotting using the indicated anti-MCM antibodies. (A) Coimmunoprecipitations were performed in RIPA buffer containing 0.1% deoxycholate. Arrows indicate the position of the full-length MCM protein being probed for. (B) Coimmunoprecipitations were performed in RIPA buffer containing 0.5% deoxycholate.

RESULTS

Composition of MCM complexes in human cells. In order to analyze the composition of MCM complexes in human cells, we expressed two of the core MCM subunits, MCM6 and MCM7, individually in human cells fused to a C-terminal TAP tag. The tagged proteins were then isolated from whole-cell extracts on IgG resin, released from the resin by tobacco etch virus cleavage, and further purified by binding to calmodulin resin. Eluates from the calmodulin resin for TAP-MCM6 and TAP-MCM7 (Fig. 1A) were analyzed by SDS-PAGE, followed by silver staining and MALDI-TOF mass spectrometry of excised bands. In both cases, the expected interactions with the other MCM core proteins were observed, and MCM2 was also clearly seen in the complex. In TAP-MCM6 samples, bands corresponding to MCM3 and MCM5 were also apparent. For TAP-MCM7, MCM3 and MCM5 may also have been present but would have run at the same position as MCM6 and TAP-MCM7, respectively, and, hence, would not be seen. In addition to the expected MCM bands, a prominent band was observed at approximately 65 kDa in both TAP-MCM6 and TAP-MCM7 experiments. This band was identified by MALDI-TOF mass spectrometry as MGC2809, a previously unstudied protein, and was named MCM-BP. Bands at approximately 50 kDa were identified as proteolytic products of MCM-BP.

To gain further insight into the protein interactions mediated by MCM-BP in human cells and the specificity of the MCM interactions, we performed the TAP-tagging experiment in reverse by expressing full-length MCM-BP fused to a TAP tag in human cells. MCM subunits 3, 4, 5, 6, and 7 were all found to copurify with TAP-MCM-BP on IgG and calmodulin columns, while no other proteins were present in sufficient quantities for MALDI identification (Fig. 1B). This confirmed that MCM-BP interacts specifically and approximately stoichiometrically with MCM proteins. However, the MCM2 protein was not observed in the MCM complex containing TAP-MCM-BP. One interpretation of these results is that MCM-BP replaces MCM2 in the hexameric MCM complex and that both MCM-BP and MCM2 are seen when core MCM subunits are TAP tagged because there are two MCM complexes present, one containing MCM-BP and the other containing MCM2. If correct, this would predict that MCM-BP would not be recovered in the MCM complex isolated by TAP tagging of MCM2.

We then compared the complexes formed with MCM-BP and MCM2 in human cells by expressing SPA-tagged versions of MCM-BP or MCM2 in cells and isolating the complexes on anti-FLAG and calmodulin resin. The SPA tag was used since its smaller size (relative to a TAP tag) would minimize any disruption of interactions due to the tag. In both cases, MCM3, -4, -6, and -7 were recovered and identified by MALDI, but MCM-BP was not seen in the TAP-MCM2 complex, nor was MCM2 seen in the TAP-MCM-BP complex (Fig. 1C). These results were confirmed by Western blotting. Surprisingly MCM5, which was seen as a prominent band in the MCM-BP complex, was considerably reduced in the MCM2 complex. The results suggest that MCM-BP can take the place of MCM2 in an MCM complex and that MCM5 is more tightly associated with the MCM-BP-containing complex than the MCM2-containing complex.

We next performed coimmunoprecipitation experiments in order to verify that the MCM-BP-containing complexes were not driven by overexpression of the tagged MCM subunit. To this end, endogenous MCM-BP was immunoprecipitated with antibodies raised against purified MCM-BP and affinity purified from rabbit immune serum. Western blots verified that the MCM4 and MCM6 core subunits coprecipitated with MCM-BP, while MCM2 was not observed (Fig. 2A). As expected, MCM4 and MCM6 also coimmunoprecipitated with MCM2, while MCM-BP did not. Therefore, coimmunoprecipitation experiments are consistent with the idea that MCM-BP and MCM2 form distinct MCM complexes in human cells.

We also performed coimmunoprecipitation experiments under more stringent conditions (by increasing the concentration of

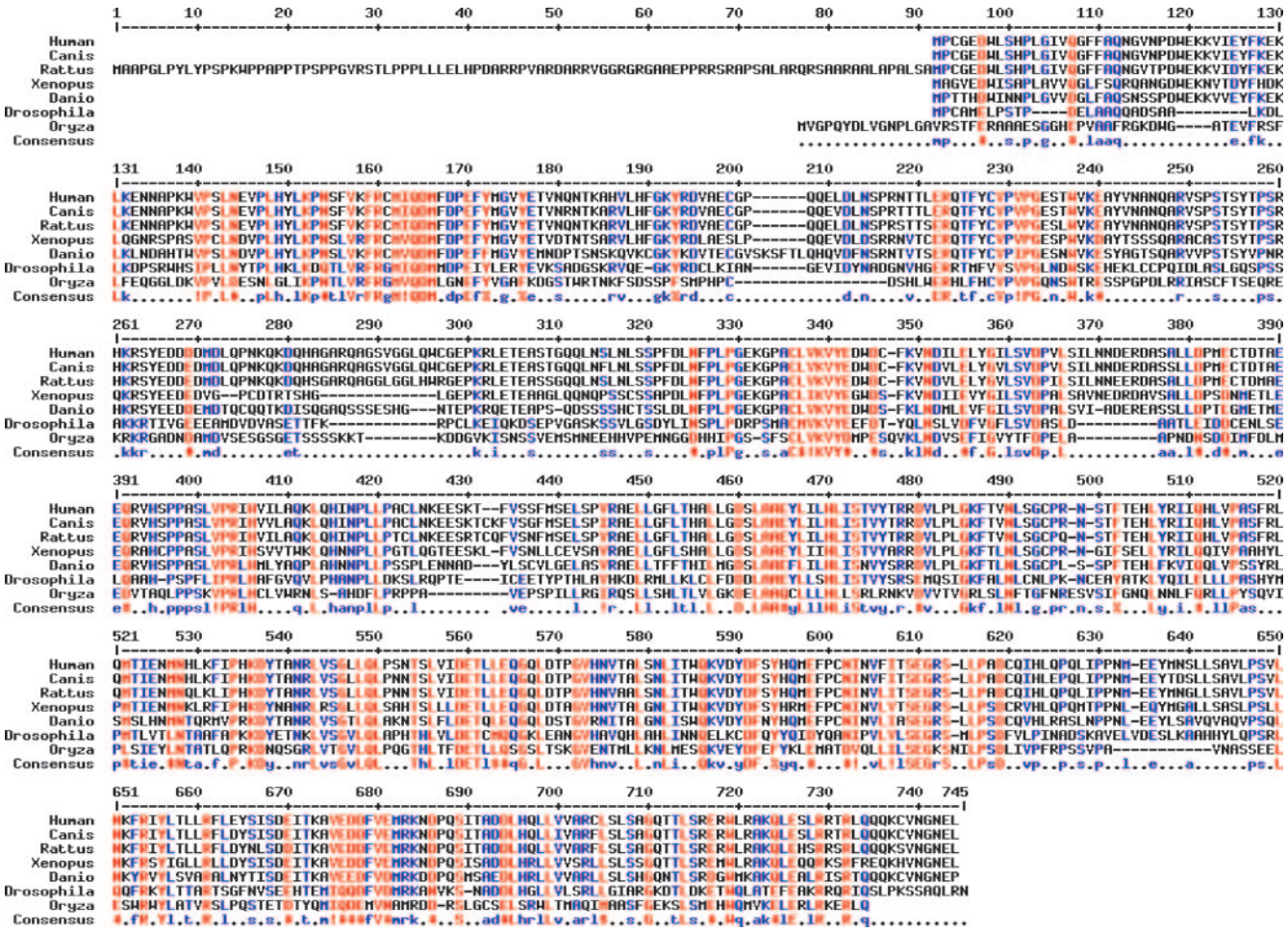

FIG. 3. MCM-BP homologues. The protein sequence of MCM-BP was aligned to homologues from *Canis familiaris* (gene identifier [GI], 73998920), *Rattus norvegicus* (GI, 62641371), *Xenopus laevis* (GI, 27769125), *Danio rerio* (GI, 68371179), *Drosophila melanogaster* (GI, 24582378) and *Oryza sativa* (GI, 55770524) using MultAlin at INRA (3).

deoxycholate from 0.1 to 0.5%), which have been reported to disrupt the association of MCM2 with the MCM complex without disrupting the MCM4/6/7 core complex (36). As expected, no MCM proteins were observed to precipitate with MCM2 under these conditions, while immunoprecipitation of MCM7 confirmed that interactions still occurred between the core subunits (Fig. 2B). Interestingly, MCM-BP was also found to coimmunoprecipitate with MCM7 and, conversely, MCM3-7 coimmunoprecipitated with MCM-BP, indicating that the MCM-BP-containing MCM complex is more stable than the MCM2-containing complex.

Sequence analysis of MCM-BP. Blast analysis of human MCM-BP revealed homologues in most multicellular eukaryotes with the exception of *Caenorhabditis elegans*. There were no obvious homologues of MCM-BP in yeast. The alignment in Fig. 3 shows that MCM-BP is highly conserved in mammals, frogs, fish, flies, and rice, although this gene product has not been studied in any of these systems. We also aligned MCM-BP with human MCM proteins. MCM-BP shares little homology with MCM proteins, including the MCM box. While MCM-BP lacks the Walker A and arginine finger motifs of MCM2-8, it does contain a 15-amino-acid region of homology with MCM4/6/7 that overlaps with the Walker B sequence (Fig. 4A). Reiterative PSI-BLAST analyses also identify limited homology of the MCM-BP C-terminal region with MCM proteins from a variety of organisms including *Archaea*, particularly with MCM7 (Fig. 4B). Therefore, MCM-BP appears to be distantly related to MCM proteins.

Interactions of MCM-BP with MCM complexes in vitro. Since our results indicated that MCM-BP can form a stable complex with MCM3-7 in human cells, we asked whether this complex could be reconstituted by coexpression of these proteins in insect cells. To this end, FLAG-tagged MCM7 was coexpressed with MCM3-6 and either MCM-BP or MCM2 (all of which lack FLAG tags); then, MCM7 and associated proteins were isolated on anti-FLAG resin. In keeping with the TAP-tagging results, MCM-BP was recovered in complex with MCM3-7 and in similar quantities as MCM2 in the MCM2-7 complex (Fig. 5A). Since several of the MCM subunits comigrate in this gel system, we also performed Western blotting on equal amounts of the FLAG eluates for the individual MCM subunits to assess their recovery. While MCM subunits 3, 4, and 6 were clearly present in both MCM2-containing and MCM-BP-containing complexes, very little MCM5 was recov-

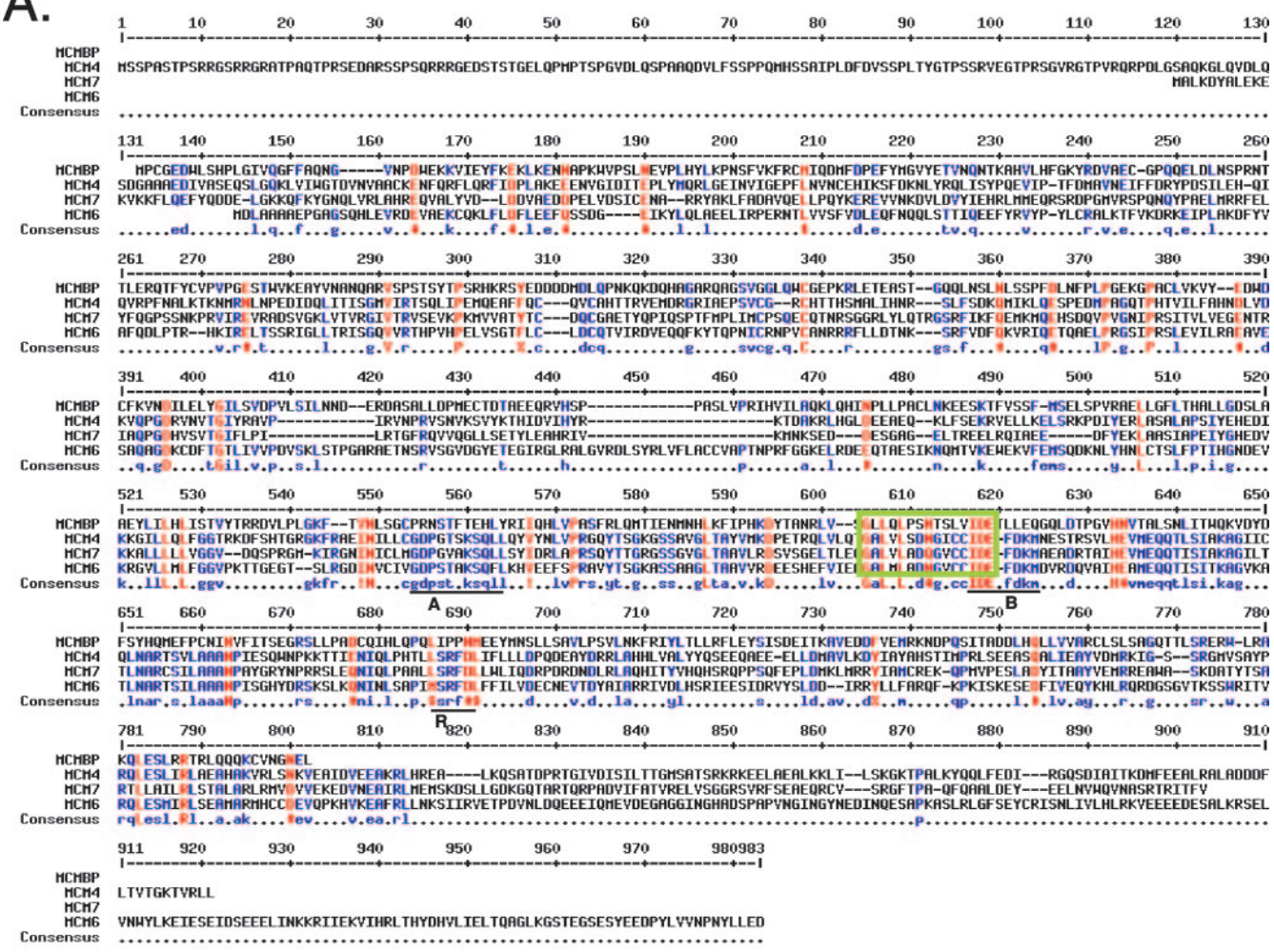

FIG. 4. Sequence similarities of MCM-BP with other MCM proteins. (A) Alignment of MCM-BP with human MCM core subunits using MultAlin at INRA. A region of homology is indicated by the green box. The Walker A (A), Walker B (B), and R-finger (R) motifs conserved in MCM proteins are underlined. (B) Examples of reiterative PSI-BLAST hits with MCM7 proteins from humans, *Xenopus laevis*, and *Danio rerio* and with the MCM protein from *Sulfolobus acidocaldarius*. MultAlin sequence alignment of the C-terminal portion of these proteins with the C terminus of MCM-BP is shown.

ered in the MCM2-containing complex compared to the MCM-BP-containing complex (Fig. 5A). This is consistent with the TAP-tagging results, indicating that MCM5 is more stably associated with MCM complexes containing MCM-BP than MCM2.

Since MCM2 can interact with the MCM4/6/7 core helicase complex in the absence of MCM3 and MCM5, we asked whether MCM-BP could also interact with the core helicase complex. In one set of experiments, MCM-BP was coexpressed in insect cells with MCM4, MCM6, and FLAG-tagged MCM7; in another, MCM-BP was expressed separately in insect cells and then mixed with insect cell lysates where MCM4, MCM6, and FLAG-MCM7 had been coexpressed. In both cases, MCM-BP was recovered on anti-FLAG resin along with

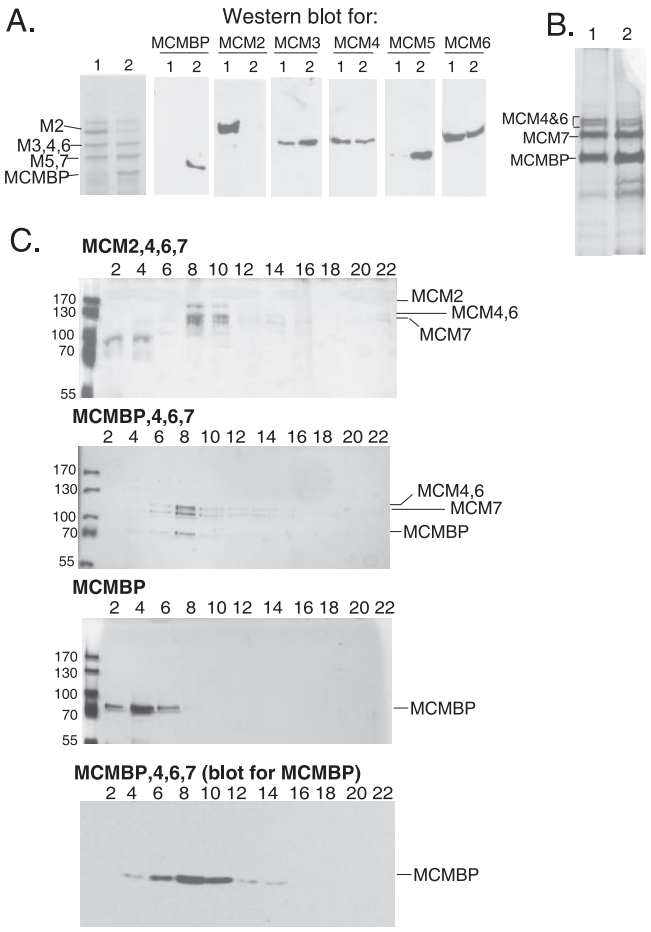

FIG. 5. Interactions of MCM-BP with recombinant MCM proteins. (A) FLAG-tagged MCM7 was coexpressed in insect cells with MCM2-6 (lanes 1) or MCM3-6 and MCM-BP (lanes 2), all of which lack FLAG tags. MCM7 and interacting proteins were isolated on anti-FLAG resin and then analyzed by SDS-PAGE and silver staining (far left lanes). Equivalent amounts of the two samples were also analyzed by Western blotting using antibodies specific for each MCM as indicated. (B) FLAG-tagged MCM7 was coexpressed in insect cells with MCM4 and MCM6 with (lane 1) or without (lane 2) MCM-BP. Lysates containing MCM4/6/7 and MCM-BP were applied to anti-FLAG resin (lane 1). Lysates containing MCM4/6/7 were mixed with insect cell lysates containing MCM-BP and then applied to anti-FLAG resin (lane 2). Eluates from the anti-FLAG resin were analyzed by SDS-PAGE and silver staining, and band identities were confirmed by mass spectrometry. (C) Complexes of MCM2/4/6/7 (first panel) or MCM-BP with MCM4/6/7 (second and fourth panels) were generated and purified as described in Materials and Methods and then analyzed by glycerol gradient sedimentation, as was MCM-BP alone (third panel). Equal volumes of every second gradient fraction were examined by SDS-PAGE and silver staining and fractions of the MCM-BP/4/6/7 gradient were also analyzed by immunoblotting using anti-MCM-BP antibodies (fourth panel). The glycerol gradient standards aldolase (158 kDa), catalase (232 kDa), ferritin (440 kDa), and thyroglobulin (670 kDa) peaked at fractions 6, 8, 10, and 12, respectively (data not shown).

MCM4, -6, and -7 (Fig. 5B), indicating that MCM-BP can interact with the core complex in the absence of MCM3 and MCM5. Glycerol gradient sedimentation analysis of the complex comprised of MCM-BP and MCM4/6/7 (MCB-BP/4/6/7) confirmed that MCM-BP cosedimented with MCM4, -6, and -7 (Fig. 5C) and was similar in size to the tetrameric MCM2/4/6/7 complex (both complexes peaking a fraction 8). The presence of MCM-BP in this complex was confirmed by Western blotting of the gradient fractions (Fig. 5C, bottom panel). In contrast, MCM-BP on its own migrated at a position consistent with a monomeric species (Fig. 5C, third panel). This glycerol gradient analysis was performed under higher salt concentrations (100 mM NaCl) than used for helicase assays in order to detect more stable complexes. Under the low-salt conditions used for helicase assays, MCM4/6/7 formed both trimeric and larger complexes and, when present, MCM-BP but not MCM2 was observed in the larger complexes (data not shown). However, aggregation of the MCM4/6/7 complexes was also evident under these conditions, precluding accurate assessment of the larger complexes.

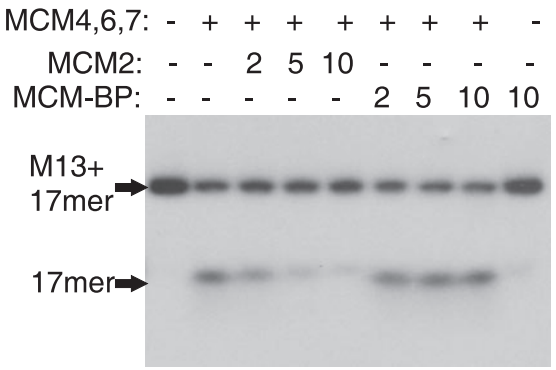

FIG. 6. MCM-BP does not inhibit the helicase activity of MCM4/6/7. DNA helicase assays were performed for 1 h using a constant amount of highly purified MCM4/6/7 complex with or without 2, 5, or 10 pmol of purified MCM2 or purified MCM-BP as indicated. The displacement of an end-labeled 17-mer from single-stranded M13 DNA was measured by PAGE and autoradiography.

MCM-BP does not inhibit the helicase activity of MCM4/6/7. MCM4/6/7 is the only MCM complex reported to have DNA helicase activity in vitro, and MCM2 is known to inhibit this helicase activity. Since MCM-BP can replace MCM2 in the MCM complex, we asked whether MCM-BP affected the helicase activity of MCM4/6/7. The MCM4/6/7 complex was generated by coexpressing these subunits in insect cells and was purified extensively by virtue of affinity tags on the subunits. Helicase assays were performed with fixed amounts of the MCM4/6/7 complex and increasing amounts of purified MCM2 or MCM-BP, and displacement of an end-labeled 17-mer oligonucleotide from M13 single-stranded DNA was measured as described previously (12) (Fig. 6). As expected, MCM2 inhibited the helicase activity of MCM4/6/7; however, the helicase activity was not affected by the addition of MCM-BP. MCM-BP was also tested for helicase activity on its own, but none was observed (Fig. 6, last lane). Therefore, unlike MCM2, MCM-BP does not inhibit the helicase activity of the MCM complex.

MCM-BP associates with chromatin in a cell cycle-dependent manner. Affinity-purified antibodies against MCM-BP were used to examine the cellular localization of endogenous MCM-BP by immunofluorescence microscopy. MCM-BP showed extensive nuclear staining in human cells, similar to MCM subunits (shown in comparison to MCM6 in Fig. 7A).

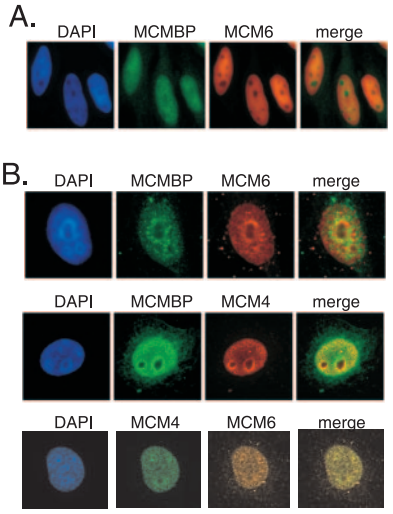

FIG. 7. Nuclear localization of MCM-BP. (A) Whole HeLa cells were fixed and stained for MCM-BP and MCM6 and counterstained with DAPI. (B) HeLa cells were extracted with Triton X-100 prior to fixing and staining for MCM-BP and either MCM6 or MCM4, as indicated, or stained for MCM4 and MCM6 (bottom). Images were captured by immunofluorescence microscopy using identical exposure times. Overlays of the two stained images are also shown (merge).

After Triton X-100 extraction, a proportion of MCM-BP was seen to be associated with the chromatin, a fraction of which overlaps with MCM subunits (shown in comparison to MCM4 and MCM6 in Fig. 7B). For comparison, the degree of overlap of MCM4 and MCM6 in Triton X-100-extracted cell is also shown (Fig. 7B, bottom panel).

We also examined the association of MCM-BP with chromatin through the cell cycle by biochemical fractionation. To this end, HeLa cells were blocked in G_1/S with aphidicolin or in G_2 or early M phase with nocodazole. G_2- and early-M-phase cells were then separated by mitotic shake-off as previously described (2). S-phase cells were also generated by 3-h release of G_1/S cells from the aphidicolin block, and late-M-phase cells were generated by 3-h release of early M cells from the nocodazole block. Cell cycle stages were confirmed by fluorescence-activated cell sorting analysis (data not shown). Cells lysates were separated into soluble and nuclear pellet fractions, the latter of which were extracted to release chromosomal proteins. Equal amounts of chromatin-bound protein were then used in Western blotting to follow endogenous MCM-BP and compared to endogenous MCM4 and MCM6 (Fig. 8A). Like MCM4 and MCM6, MCM-BP was found to have the highest association with chromatin in G_1/S and S samples, reduced binding to chromatin in G_2, and further decreased binding in early-M-phase samples. It then reassociated with the chromatin in late M phase. However, a larger fraction of MCM-BP appeared to be on the chromatin in G_2 compared to that for MCM4 or MCM6, suggesting that MCM-BP dissociates from the chromatin slightly later than other MCM proteins. A quantitative summary of multiple experiments is shown in Fig. 8B. We conclude that a proportion of MCM-BP associates with chromatin in a cell cycle-dependent manner similar to that of the MCM complex.

We also followed MCM-BP- and MCM2-containing MCM complexes throughout the cell cycle by immunoprecipitating MCM-BP or MCM2 from chromatin or soluble cellular fractions (Fig. 8C). Both MCM2 and MCM-BP were observed to form a complex with MCM4 in chromatin fractions from G_1/S (aphidicolin blocked) through S (3- and 6-h release from aphidicolin) and G_2 (9-h release from aphidicolin) phases but were not detected or were greatly reduced in the chromatin fraction in early-M-phase cells (nocodazole blocked), consistent with the results shown in Fig. 8A and B. Interestingly, while MCM2 also bound MCM4 in the soluble fraction, there was little interaction between soluble MCM-BP and MCM4, suggesting that MCM-BP-containing MCM complexes are preferentially formed on chromatin. In keeping with the results shown in Fig. 1 and 2, MCM2 and MCM-BP were never observed to interact with each other.

MCM-BP is preferentially localized to a replication origin in G_1 phase. The MCM2-7 complex is loaded onto origins of replication in mitosis remaining there until the onset of DNA synthesis, at which time the complex moves away from the origins with the replication forks. We asked whether MCM-BP behaved similarly by performing ChIP experiments on the LB2 replicon. Antibodies against MCM-BP, MCM2, and MCM4 were used, in addition to normal rabbit control antibodies, and recovered DNA fragments were assessed by quantitative PCR. Consistent with previous reports, the MCM proteins were preferentially associated with the LB2 origin fragment in G_1, compared to DNA fragments located approximately 3 or 4 kb away from the origin (on opposite sides of the origin), but the proteins were more equally distributed on the two fragments in S phase. Composite results from multiple experiments are shown in Fig. 8D. The same trend was seen for MCM-BP, which gave results very similar to those for MCM2, indicating that MCM-BP is preferentially loaded at this origin of replication but has decreased association with the origin in S phase. While MCM4 consistently gave a stronger signal on the origin (in G_1) than either MCM2 or MCM-BP, this was accompanied by increased recovery of the distant DNA fragments so that the degree of specificity of MCM4 for the origin was approximately the same as for MCM2 and MCM-BP.

Effects of down-regulation of MCM-BP. To further assess the role of MCM-BP in human cells, we attempted to silence MCM-BP expression by siRNA. This treatment significantly down-regulated cellular levels of MCM-BP but did not completely silence MCM-BP; in particular, some chromatin-bound MCM-BP remained after siRNA treatment (Fig. 9A, lanes 7 and 8, and B, lanes 3 and 4). This might account for the lack of major effects seen on cell growth and total bromodeoxyuridine incorporation after MCM-BP siRNA treatment (data not shown). However, down-regulation of MCM-BP was consistently found to decrease the association of MCM4 with cellular chromatin at G_1/S. The level of chromatin-bound MCM4 was typically higher in aphidicolin-blocked cells than in asynchronous cells (compare lanes 5 and 6 in Fig. 9A and lanes 1 and 2 in B); however, after silencing MCM-BP, the increased chromatin association of MCM4 at G_1/S was not observed (Fig. 9A, compare lanes 7 and 8, and B, compare lanes 3 and 4). The decrease in chromatin-bound MCM4 upon down-regulation of MCM-BP was accompanied by an increase in soluble MCM4 (Fig. 9A, compare lanes 2 and 4), suggesting that MCM-BP is important for either the loading or the stabilization of MCM4

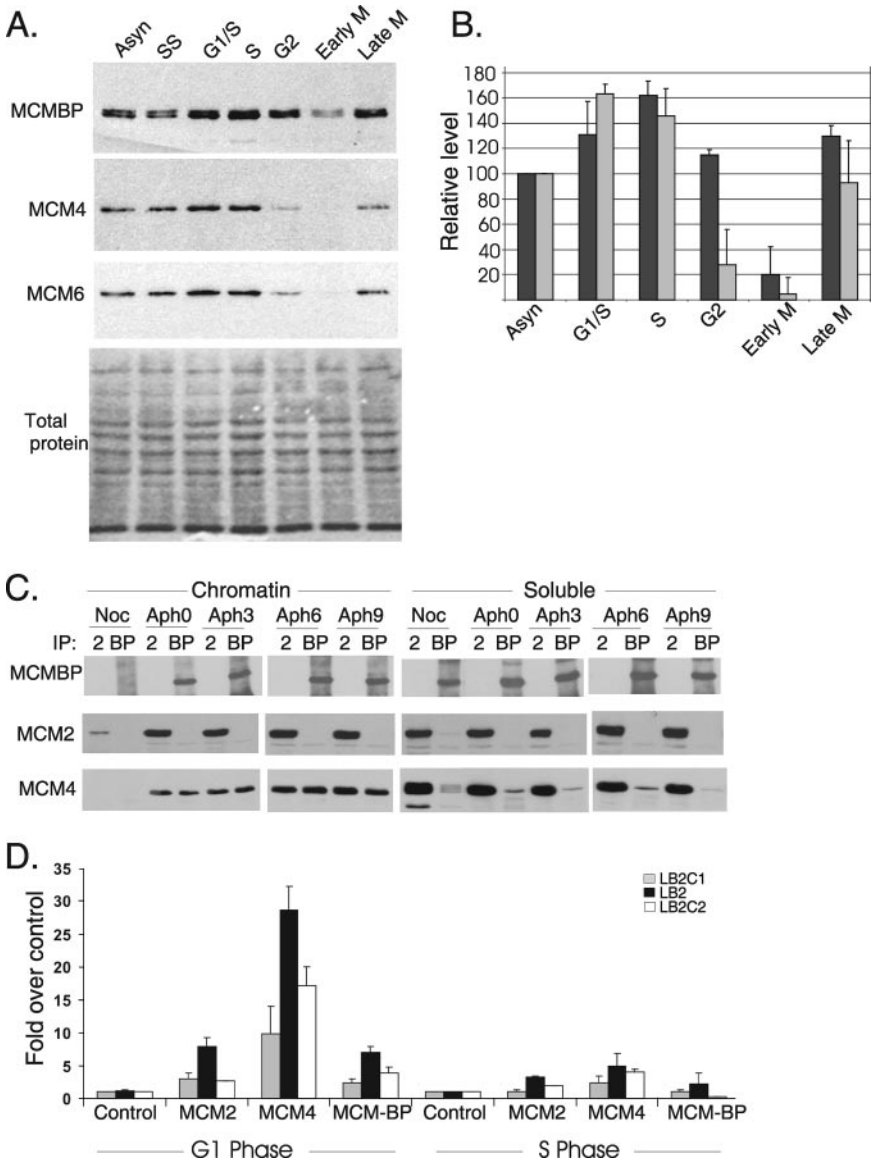

FIG. 8. Association of MCM-BP with cellular chromatin. HeLa cells at the indicated points in the cell cycle were biochemically fractionated to generate soluble and chromatin-bound protein fractions. Equal amounts of protein from each sample were compared by SDS-PAGE and Western blotting for MCM-BP, MCM4, MCM6, or MCM2 as indicated. (A) Chromatin-bound fractions are shown from asynchronous (Asyn), serum-starved (SS), or synchronous cells at the indicated point in the cell cycle. The bottom panel is the ponceau-S-stained membrane showing equal protein loading. (B) Average levels of chromatin-bound MCM-BP (black) and MCM4 (gray) from three experiments are shown relative to those in asynchronous (Asyn) cells. (C) Cells were blocked in early M (Noc) or at G_1/S (Aph0), and G_1/S cells were released from the block for 3 (Aph3), 6 (Aph6), or 9 (Aph9) h. Fluorescence-activated cell sorting analysis indicated that Aph3 and Aph6 cells were in S and Aph9 cells were in G_2 (data not shown). Cell extracts were separated into chromatin and soluble fractions, and each fraction was incubated with antibody against either MCM-BP (BP) or MCM2 (2). Immunoprecipitants were then Western blotted for MCM-BP, MCM2, and MCM4. (D) Chromatin immunoprecipitations were performed on cells in G_1 or S phase, using antibodies against MCM-BP, MCM2, and MCM4 or negative control rabbit antibodies (control). Recoveries of the fragment corresponding to the LB2 origin (black), a fragment 4 kb away from the origin (LB2C1; gray), and a fragment 3 kb away from the origin on the opposite site (LB2C2; white) were then determined by quantitative PCR, normalized to the input sample, and shown as the relative increase (*n*-fold) over control antibodies. Average values from multiple experiments are shown along with standard deviations.

on chromatin. MCM-BP silencing did not have an obvious effect on the chromatin association of other MCM subunits. A summary of the effects of MCM-BP silencing on soluble and chromatin-bound MCM4 and MCM6 at G_1/S phase is shown in Fig. 9C.

Effects of down-regulation of MCM4 and cdc6 on MCM-BP chromatin loading. We also asked whether the loading of MCM-BP on chromatin was dependent on MCM4 as well as on the cdc6 protein known to be required for the loading of MCM complexes on chromatin (5). Down-regulation of either MCM4 or cdc6 by siRNA consistently caused a twofold decrease in the amount of MCM-BP on chromosomes (Fig. 9D). The chromatin association of MCM6 (in MCM4 silencing experiments) or MCM4 (in cdc6 silencing experiments) was af-

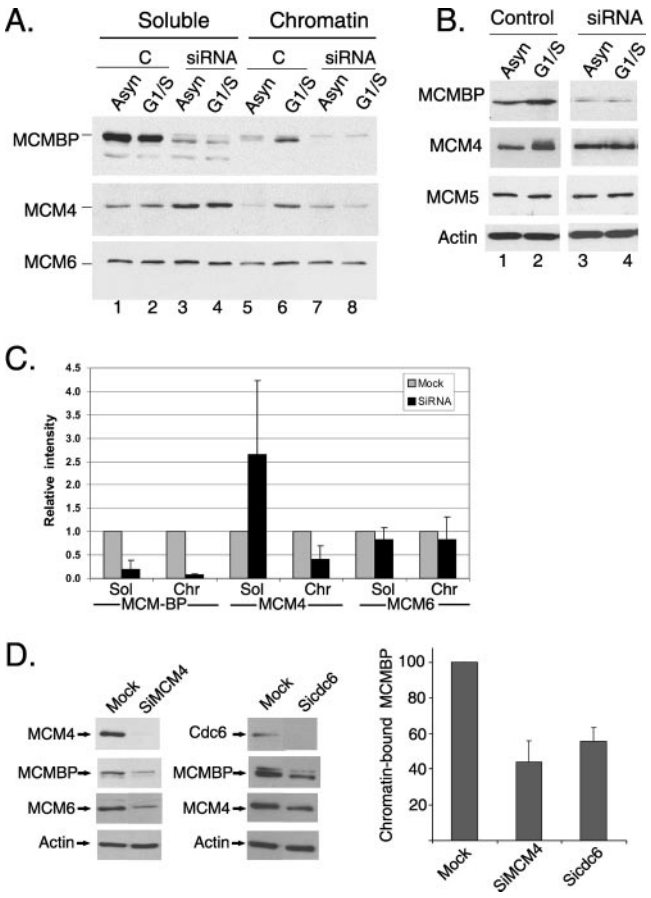

FIG. 9. MCM-BP silencing affects the chromatin association of MCM4 and vice versa. (A to C) HeLa cells were transfected with siRNA against MCM-BP (siRNA) or GFP (C or control) and then were either left asynchronous (Asyn) or blocked at G_1/S with aphidicolin (G1/S). Cells were then lysed and separated into soluble and chromatin-bound (chromatin) fractions. Equal amounts of soluble or chromatin-bound fractions were analyzed by SDS-PAGE and immunoblotted with antibodies specific for MCM-BP, MCM4, MCM5, MCM6, or actin as indicated. The experiments shown in panels A and B are independent. Only the chromatin-bound fractions are shown in panel B. (C) The average intensity of the indicated MCM bands in soluble (Sol) and chromatin (Chr) fractions in G_1/S cells is shown (from three experiments) after treatment with MCM-BP siRNA (black) or mock treatment with GFP siRNA (gray). Bands were normalized to the actin loading control, and MCM-BP-silenced samples are shown relative to the mock-treated sample (set to 1). (D) HeLa cells were transfected with siRNA against MCM4 (SiMCM4), cdc6 (Sicdc6), or GFP (mock). Two days later, chromatin fractions were prepared, and equal amounts of each fraction were analyzed by Western blotting with antibodies against MCM4, MCM-BP, MCM6, or actin. For cdc6 silencing, a cdc6 immunoblot of whole cell lysates is also shown (top panel). The right panel is the quantification of the MCM-BP band from three experiments relative to the mock treatment.

fected to a similar degree. The results are consistent with a significant proportion of MCM-BP's being loaded onto chromosomes as part of the MCM complex.

DISCUSSION

We have identified a new component of the human MCM complex that is conserved in most multicellular eukaryotes. To date, MCM subunits have been identified either due to their requirement for minichromosome maintenance in yeast (25) or due to sequence homology, particularly in the MCM box. However, these approaches may not have identified MCM-BP, as close homologues of MCM-BP appear to be lacking in yeast, and the very limited homology to MCM subunits would have hampered its identification by sequence analysis. Since MCM-BP did not adhere to the previous criteria for MCM proteins, we felt that it was more aptly named MCM-BP rather than giving it an MCM number.

Since the discovery of the MCM2-7 complex, three additional MCM proteins (MCM8, -9, and -10) have been identified. However, unlike MCM-BP, MCM8, MCM9, and MCM10 have not been found to stably interact with the MCM complex or any of the MCM subunits. Like MCM-BP, neither MCM8 nor MCM9 is present in yeast (27). The phylogenetic distribution of MCM-BP is much like that of MCM8, as both proteins are present in most multicellular eukaryotes but lack obvious homologues in *C. elegans*.

Our data indicate that MCM-BP interacts quite strongly and specifically with MCM complexes. Like MCM2, MCM-BP purifies in complex with MCM3-7; however, MCM-BP and MCM2 have not been observed in the same complex, suggesting that one prevents the interaction of the other with the MCM complex. Since MCM2-7 has been reported to form a hexamer, the simplest interpretation is that MCM-BP may replace MCM2 to form a hexamer with MCM3-7. However, additional analyses are required to accurately determine the nature of the MCM-BP-containing complex. We have also found that, like MCM2, MCM-BP can stably interact with the MCM4/6/7 core helicase complex, giving a complex that migrates at a similar position as the MCM2/4/6/7 tetramer in a glycerol gradient. However, unlike MCM2, the interaction of MCM-BP with the core helicase did not inhibit its helicase activity. Since replicative helicases are hexameric, it is unlikely that the active helicase containing MCM-BP is the MCM-BP/MCM4/6/7 tetramer seen on the glycerol gradient under high-salt conditions. Rather, it is more likely to be a larger complex of these subunits, which can form under the low-salt conditions of the helicase assay.

Immunoprecipitation of endogenous MCM-BP or MCM2 under different conditions revealed that MCM-BP-containing MCM complexes are more stable than those containing MCM2. The individual subunit interactions observed for MCM proteins in both *S. cerevisiae* and humans point to a model where MCM2 bridges the interaction between the MCM4/6/7 core complex and MCM3 and MCM5 (predominantly through MCM5) (6, 35, 38, 40). If MCM-BP replaced MCM2 in this complex but made stronger contacts with the core and MCM5, then a more stable hexameric complex would result, consistent with our observations. In both the SPA-tagging experiments in human cells and reconstitution experiments in insect cells, we observed that the MCM5 interaction with the MCM2-containing complex was particularly labile in comparison to that in the MCM-BP-containing complex. This might reflect a direct interaction of MCM-BP with MCM5 in the complex, as is predicted for MCM2, but could be due to other structural differences in the MCM-BP- and MCM2-containing complexes. It is also possible that the reduced association of MCM5 with the MCM2 complex is due to disruption of this interaction by the C-terminal purification tags on MCM2; however, this seems unlikely since tags on either end of yeast MCM

proteins have not been found to have any effect on complex formation or biochemical activities (35). In either case, our results suggest that MCM5 can dissociate from the MCM2 complex independently from MCM3, since MCM3 levels were similar in MCM2- and MCM-BP-containing complexes.

Like the MCM2-7 subunits, MCM-BP was found throughout the nucleus, in both the soluble and chromatin-bound fractions. In human cells, the MCM subunits assemble on DNA beginning in late mitosis and remain associated with the chromatin until early G_2, after DNA synthesis is completed (11, 18, 37). MCM proteins have also been shown to be preferentially loaded at human origins of replication and then distributed to more distal sequences during DNA synthesis (16, 34). A similar pattern of cell cycle-dependent chromosome and origin association was observed for MCM-BP, consistent with the possibility that some MCM-BP is loaded onto DNA as part of an MCM complex. The decreased association of MCM-BP with chromatin after down-regulation of MCM4 or cdc6 also supports this hypothesis, as does the observation that MCM4 readily coimmunoprecipitates with MCM-BP from chromatin fractions but does so much less efficiently from soluble protein fractions. Dissociation of MCM-BP from the chromatin appears to occur slightly later in the cell cycle (early M as opposed to G_2 phase) than for the other MCM subunits, which could be interpreted in two ways. First, the MCM-BP-containing MCM complexes could disassemble in G_2 in such a way that the MCM subunits dissociate from the chromatin while MCM-BP remains chromatin bound. Second, the MCM-BP-containing MCM complexes may remain intact and dissociate from the chromatin in G_2/early M phase, slightly later than the MCM2-containing complexes. This would result in the observed decreased levels of MCM4 and MCM6 on the chromatin in G_2, as only the fraction of these proteins that are in the MCM-BP complexes would remain on the chromatin.

MCM-BP may contribute to the loading or stabilization of some MCM complexes on chromatin as down-regulation of MCM-BP reduced the amount of MCM4 present in the chromatin fraction at G_1/S. Similar effects were not observed on MCM6 or MCM7 (data not shown), suggesting that some MCM4 may move on or off chromatin independently of the core helicase complex. While MCM4, -6, and -7 are generally thought to function as a complex, at least two other studies in human cells have found that MCM4 can act independently from MCM6 and MCM7 (16, 19). MCM4 has also been shown to assemble on chromatin independently from MCM2 and MCM3 in *Xenopus* egg extracts (4).

In summary, we have identified an alternative MCM complex to the classically described MCM2-7 hexamer, where MCM2 is replaced by MCM-BP. This is reminiscent of the alternative forms of replication factor C (RFC) complexes that have been identified, where the RFC1 subunit of the pentameric complex can be replaced by Ctf18, Rad24, or Elg1 (1, 15). These alternative RFC complexes contribute to the maintenance of genome integrity under conditions of cellular stress. It is not yet clear whether the MCM-BP-containing MCM complex makes a consistent contribution to DNA replication (perhaps in concert with MCM2 complexes) or primarily functions in particular circumstances such as cellular stress responses. Further studies will be necessary to determine the precise contribution of MCM-BP to MCM protein functions.

ACKNOWLEDGMENTS

We gratefully acknowledge Jack Greenblatt and Mahel Zeghouf for pMZI and pMZS3F vectors. We also thank Rolf Knippers and Masahide Ishibashi for cDNA clones of human MCM6 and MCM7, respectively, and Grant Brown for critical reading of the manuscript.

This work was supported by a grant from the Canadian Institutes of Health Research (CIHR) to L.F. and by a CIHR postdoctoral fellowship to A.M.S. L.F. is a Canada Research Chair in Molecular Virology.

REFERENCES

1. **Aroya, S. B., and M. Kupiec.** 2005. The Elg1 replication factor C-like complex: a novel guardian of genome stability. DNA Repair **4:**409–417.
2. **Ballabeni, A., M. Melixetian, R. Zamponi, L. Masiero, F. Marinoni, and K. Helin.** 2004. Human geminin promotes pre-RC formation and DNA replication by stabilizing CDT1 in mitosis. EMBO J. **23:**3122–3132.
3. **Corpet, F.** 1988. Multiple sequence alignment with hierarchical clustering. Nucleic Acids Res. **16:**10881–10890.
4. **Coue, M., F. Amariglio, D. Maiorano, S. Bocquet, and M. Mechali.** 1998. Evidence for different MCM subcomplexes with differential binding to chromatin in *Xenopus*. Exp. Cell Res. **245:**282–289.
5. **Cvetic, C. A., and J. C. Walter.** 2006. Getting a grip on licensing: mechanism of stable Mcm2-7 loading onto replication origins. Mol. Cell **21:**143–144.
6. **Davey, M. J., C. Indiani, and M. O'Donnell.** 2003. Reconstitution of the Mcm2-7p heterohexamer, subunit arrangement, and ATP site architecture. J. Biol. Chem. **278:**4491–4499.
7. **Fien, K., and J. Hurwitz.** 2006. Fission yeast Mcm10p contains primase activity. J. Biol. Chem.
8. **Forsburg, S. L.** 2004. Eukaryotic MCM proteins: beyond replication initiation. Microbiol. Mol. Biol Rev. **68:**109–131.
9. **Gozuacik, D., M. Chami, D. Lagorce, J. Faivre, Y. Murakami, O. Poch, E. Biermann, R. Knippers, C. Brechot, and P. Paterlini-Brechot.** 2003. Identification and functional characterization of a new member of the human Mcm protein family: hMcm8. Nucleic Acids Res. **31:**570–579.
10. **Holowaty, M. N., M. Zeghouf, H. Wu, J. Tellam, V. Athanasopoulos, J. Greenblatt, and L. Frappier.** 2003. Protein profiling with Epstein-Barr nuclear antigen 1 reveals an interaction with the herpesvirus-associated ubiquitin-specific protease HAUSP/USP7. J. Biol. Chem. **278:**29987–29994.
11. **Holthoff, H. P., M. Baack, A. Richter, M. Ritzi, and R. Knippers.** 1998. Human protein MCM6 on HeLa cell chromatin. J. Biol. Chem. **273:**7320–7325.
12. **Ishimi, Y.** 1997. A DNA helicase activity is associated with an MCM4, -6, and -7 protein complex. J. Biol. Chem. **272:**24508–24513.
13. **Ishimi, Y., S. Ichinose, A. Omori, K. Sato, and H. Kimura.** 1996. Binding of human minichromosome maintenance proteins with histone H3. J. Biol. Chem. **271:**24115–24122.
14. **Johnson, E. M., Y. Kinoshita, and D. C. Daniel.** 2003. A new member of the MCM protein family encoded by the human MCM8 gene, located contrapodal to GCD10 at chromosome band 20p12.3-13. Nucleic Acids Res. **31:**2915–2925.
15. **Kim, J., and S. A. MacNeill.** 2003. Genome stability: a new member of the RFC family. Curr. Biol. **13:**R873—R875.
16. **Kinoshita, Y., and E. M. Johnson.** 2004. Site-specific loading of an MCM protein complex in a DNA replication initiation zone upstream of the c-MYC gene in the HeLa cell cycle. J. Biol. Chem. **279:**35879–35889.
17. **Koonin, E. V.** 1993. A common set of conserved motifs in a vast variety of putative nucleic acid-dependent ATPases including MCM proteins involved in the initiation of eukaryotic DNA replication. Nucleic Acids Res. **21:**2541–2547.
18. **Krude, T., C. Musahl, R. A. Laskey, and R. Knippers.** 1996. Human replication proteins hCdc21, hCdc46 and P1Mcm3 bind chromatin uniformly before S-phase and are displaced locally during DNA replication. J. Cell Sci. **109:**309–318.
19. **Kudoh, A., T. Daikoku, Y. Ishimi, Y. Kawaguchi, N. Shirata, S. Iwahori, H. Isomura, and T. Tsurumi.** 2006. Phosphorylation of MCM4 at sites inactivating DNA helicase activity of the MCM4-MCM6-MCM7 complex during Epstein-Barr virus productive replication. J. Virol. **80:**10064–10072.
20. **Labib, K., S. E. Kearsey, and J. F. Diffley.** 2001. MCM2-7 proteins are essential components of prereplicative complexes that accumulate cooperatively in the nucleus during G_1-phase and are required to establish, but not maintain, the S-phase checkpoint. Mol. Biol. Cell **12:**3658–3667.
21. **Labib, K., J. A. Tercero, and J. F. X. Diffley.** 2000. Uninterrupted MCM2-7 function required for DNA replication fork progression. Science **288:**1643–1647.
22. **Ladenburger, E. M., C. Keller, and R. Knippers.** 2002. Identification of a binding region for human origin recognition complex proteins 1 and 2 that coincides with an origin of DNA replication. Mol. Cell. Biol. **22:**1036–1048.
23. **Lee, J., and J. Hurwitz.** 2000. Isolation and characterization of various complexes of the minichromosome maintenance proteins of *Schizosaccharomyces pombe*. J. Biol. Chem. **275:**18871–18878.
24. **Lutzmann, M., D. Maiorano, and M. Mechali.** 2005. Identification of full

genes and proteins of MCM9, a novel, vertebrate-specific member of the MCM2-8 protein family. Gene **362:**51–56.
25. **Maine, G. T., P. Sinha, and B. K. Tye.** 1984. Mutants of *S. cerevisiae* defective in the maintenance of minichromosomes. Genetics **106:**365–385.
26. **Maiorano, D., O. Cuvier, E. Danis, and M. Mechali.** 2005. MCM8 is an MCM2-7-related protein that functions as a DNA helicase during replication elongation and not initiation. Cell **120:**315–328.
27. **Maiorano, D., M. Lutzmann, and M. Mechali.** 2006. MCM proteins and DNA replication. Curr. Opin. Cell Biol. **18:**130–136.
28. **Merchant, A. M., Y. Kawasaki, Y. Chen, M. Lei, and B. K. Tye.** 1997. A lesion in the DNA replication initiation factor Mcm10 induces pausing of elongation forks through chromosomal replication origins in *Saccharomyces cerevisiae*. Mol. Cell. Biol. **17:**3261–3271.
29. **Moyer, S. E., P. W. Lewis, and M. R. Botchan.** 2006. Isolation of the Cdc45/Mcm2-7/GINS (CMG) complex, a candidate for the eukaryotic DNA replication fork helicase. Proc. Natl. Acad. Sci. USA **103:**10236–10241.
30. **Prokhorova, T. A., and J. J. Blow.** 2000. Sequential MCM/P1 subcomplex assembly is required to form a heterohexamer with replication licensing activity. J. Biol. Chem. **275:**2491–2498.
31. **Ricke, R. M., and A. K. Bielinsky.** 2004. Mcm10 regulates the stability and chromatin association of DNA polymerase-alpha. Mol. Cell **16:**173–185.
32. **Rigaut, G., A. Shevchenko, B. Rutz, M. Wilm, M. Mann, and B. Seraphin.** 1999. A generic protein purification method for protein complex characterization and proteome exploration. Nat. Biotechnol. **17:**1030–1032.
33. **Ritzi, M., K. Tillack, J. Gerhardt, E. Ott, S. Humme, E. Kremmer, W. Hammerschmidt, and A. Schepers.** 2003. Complex protein-DNA dynamics at the latent origin of DNA replication of Epstein-Barr virus. J. Cell Sci. **116:**3971–3984.
34. **Schaarschmidt, D., E. Ladenfurger, C. Keller, and R. Knippers.** 2002. Human Mcm proteins at a replication origin during the G1 to S phase transition. Nucleic Acids Res. **30:**4176–4185.
35. **Schwacha, A., and S. P. Bell.** 2001. Interactions between two catalytically distinct MCM subgroups are essential for coordinated ATP hydrolysis and DNA replication. Mol. Cell **8:**1093–1104.
36. **Sherman, D. A., S. G. Pasion, and S. L. Forsburg.** 1998. Multiple domains of fission yeast Cdc19p (MCM2) are required for its association with the core MCM complex. Mol. Biol. Cell **9:**1833–1845.
37. **Todorov, I. T., A. Attaran, and S. E. Kearsey.** 1995. BM28, a human member of the MCM2-3-5 family, is displaced from chromatin during DNA replication. J. Cell Biol. **129:**1433–1445.
38. **Yabuta, N., N. Kajimura, K. Mayanagi, M. Sato, T. Gotow, Y. Uchiyama, Y. Ishimi, and H. Nojima.** 2003. Mammalian Mcm2/4/6/7 complex forms a toroidal structure. Genes Cells **8:**413–421.
39. **Yoshida, K.** 2005. Identification of a novel cell-cycle-induced MCM family protein MCM9. Biochem. Biophys. Res. Commun. **331:**669–674.
40. **Yu, Z., D. Feng, and C. Liang.** 2004. Pairwise interactions of the six human MCM protein subunits. J. Mol. Biol. **340:**1197–1206.
41. **Zeghouf, M., J. Li, G. Butland, A. Borowska, V. Canadien, D. Richards, B. Beattie, A. Emili, and J. F. Greenblatt.** 2004. Sequential peptide affinity (SPA) system for the identification of mammalian and bacterial protein complexes. J. Proteome Res. **3:**463–468.